

# Light-induced detonant materials: charge-transfer complexes of tetrathiafulvalene (TTF) with hexanitrostilbene (HNS) and tetraazidoquinone (TAZQ) and their associated C—H···O hydrogen-bonded networks

Marc Fourmigué,<sup>a</sup> Kamal Boubekeur,<sup>a</sup> Patrick Batail,<sup>\*,a</sup> Joël Renouard<sup>b</sup> and Guy Jacob<sup>\*,b</sup>

<sup>a</sup> Institut des Matériaux de Nantes (IMN), CNRS-Université de Nantes, 2 rue de la Houssinière, 44072 Nantes cedex 03, France.

<sup>b</sup> Société Nationale des Poudres et Explosifs, Centre de Recherche du Bouchet, BP 2, 91710 Vert Le Petit, France.

Charge-transfer complexes of tetrathiafulvalene (TTF) with the electron-poor hexanitrostilbene (HNS) or tetraazidoquinone (TAZQ) have been isolated as single crystals in a 1 : 1 stoichiometry and their structures determined by single-crystal X-ray diffraction. TTF · TAZQ crystallises in the monoclinic system, space group  $P2_1/n$  with  $a = 8.295(1)$ ,  $b = 14.984(2)$ ,  $c = 14.984(2)$  Å,  $\beta = 96.26(1)^\circ$ , and TTF · HNS crystallises in the monoclinic system, space group  $P2_1$  with  $a = 9.193(1)$ ,  $b = 7.428(2)$ ,  $c = 18.350(2)$ ,  $\beta = 94.507(9)^\circ$ . In both compounds mixed stacks of alternating donor and acceptor molecules are identified in the  $b$  direction, together with a complex network of C—H···X (X = O, N) hydrogen-bond interactions. In TTF · TAZQ, bonds between a TTF hydrogen atom and the quinoid oxygen atom of TAZQ lead to the formation of DADA chains in the  $a + b$  and  $a - b$  directions, further crosslinked in the  $c$  direction through a C—H···N interaction. In TTF · HNS, infinite helices of alternating TTF and HNS moieties develop around the  $2_1$  axis along  $b$ . These helices are further interconnected through a C—H···O hydrogen bond between two neighbouring HNS molecules in the  $a$  direction, giving rise to layers of parallel helices in the  $ab$  plane. Optical as well as preliminary light-induced detonant properties are reported.

**Induction d'explosifs par la lumière: complexes à transfert de charge du tétrathiafulvalène (TTF) avec l'hexanitrostilbène (HNS) et la tétraazidoquinone (TAZQ) et leurs réseaux de liaisons hydrogène de type C—H···O.** Des complexes à transfert de charge du tétrathiafulvalène (TTF) avec comme accepteurs l'hexanitrostilbène (HNS) et la tétraazidoquinone (TAZQ) ont été isolés sous forme de monocristaux et leurs structures déterminées par diffraction des rayons X. TTF · TAZQ cristallise dans le système monoclinique, groupe d'espace  $P2_1/n$  avec  $a = 8.295(1)$ ,  $b = 14.984(2)$ ,  $c = 14.984(2)$  Å,  $\beta = 96.26(1)^\circ$ , TTF · HNS cristallise dans le système monoclinique, groupe d'espace  $P2_1$  avec  $a = 9.193(1)$ ,  $b = 7.428(2)$ ,  $c = 18.350(2)$ ,  $\beta = 94.507(9)^\circ$ . Dans les deux composés, des colonnes alternées de donneur et d'accepteur sont identifiées dans la direction  $b$ , complétées par un réseau complexe de liaisons hydrogène C—H···X (X = O, N). Dans TTF · TAZQ, ces liaisons entre un hydrogène du TTF et l'oxygène de la quinone induisent la formation de chaînes dans les directions  $a + b$  et  $a - b$ , chaînes réticulées dans la direction  $c$  par une interaction C—H···N. Dans TTF · HNS, des hélices alternant TTF et HNS se développent autour de l'axe  $2_1$  selon  $b$ . Ces hélices sont reliées entre elles par une liaison C—H···O entre deux molécules de HNS dans la direction  $a$ , conduisant ainsi à des plans d'hélices parallèles. Des mesures préliminaires de propriétés optiques et détonantes sont reportées.

Explosion induction of explosive materials with light sources has been investigated for a long time and predevelopment systems have already been evaluated,<sup>1,2</sup> with respect to the safety and insensitivity of the devices to external perturbations.<sup>3,4</sup> The practical usefulness of such devices requires, however, that all components are small and light enough to be easily packaged and carried and in that respect, near-infrared laser diodes appear to be the best suited light sources for the coming years.

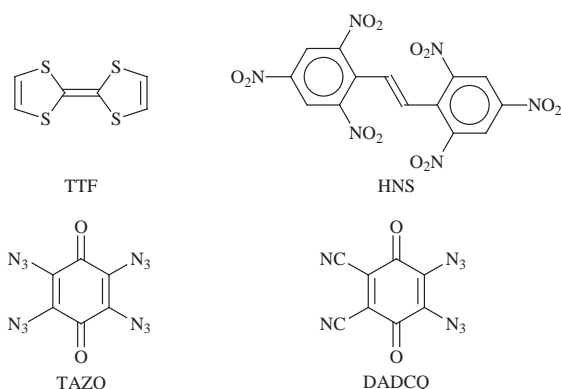
Previous work on explosive initiation with light<sup>5</sup> has shown that (i) PETN (pentaerythritol tetranitrate), lead azide and pyrotechnic firing compositions can indeed be initiated at low laser levels but at wavelengths in the UV/VIS range; (ii) secondary explosives like HMX (octogen) or RDX (hexogen) require high energy levels, incompatible with a small portable light source; and (iii) doping of primary explosives with light-absorbing substances (graphite) reduces the initiation threshold. Only CP [pentaamine(5-cyano-2H-tetrazolato)cobalt(III)]

perchlorate] and its derivatives were specifically designed for laser initiation but their sensitivity makes them less suitable for applications.<sup>6</sup> Furthermore, all known explosive materials used today absorb in the UV/VIS range while optical absorption in the red or near-IR (NIR) region would be desirable.<sup>7</sup>

Charge-transfer complexes are well-known to exhibit a strong absorption band in solution as well as in the solid state<sup>8</sup> and its energy position has been discussed by Torrance<sup>9</sup> for evaluating the degree of charge transfer and ionicity in such materials. For example, the charge-transfer absorption band is observed around 3 µm in mixed-valence TCNQ salts<sup>10</sup> but at 1.75 µm in the neutral high-temperature phase of TTF-chloranil<sup>11,12</sup> and at even higher energy in the case of weak donor and acceptor moieties. Therefore, it is tempting to take advantage of the acceptor character of several nitro-based explosive molecules like trinitrotoluene (TNT) or hexanitrostilbene (HNS) to engage them with electron-rich molecules of defined electron-donor character. Other classes

of charge-transfer salts can also be prepared from *quinones* as acceptor molecules. The substitution of two or four positions of the benzoquinone core with  $-\text{NO}_2$  or  $-\text{N}_3$  groups might also lead to interesting solid state and explosive properties of the corresponding charge-transfer complexes with TTF.

In this paper, we report on charge-transfer complexes of hexanitrostilbene (HNS), tetraazidoquinone (TAZQ) and diazidodicyanoquinone (DADCQ) with tetrathiafulvalene (TTF) as the electron-donor molecule. The structures of  $\text{TTF} \cdot \text{HNS}$  and  $\text{TTF} \cdot \text{TAZQ}$  have been analysed through the concepts of  $\pi$ - $\pi$  donor-acceptor as well as  $\text{C}-\text{H} \cdots \text{X}$  ( $\text{X} = \text{O}, \text{N}$ ) hydrogen-bond interactions. Furthermore, those complexes indeed exhibit an additional absorption band in the NIR range whose effect on the detonant properties under laser irradiation is described.



## Results and Discussion

### Synthesis and electrochemical characterization

Cyclic voltammetry experiments demonstrate that HNS and TAZQ are reversibly reduced to the radical anion at  $-0.48 \text{ V}$  and  $-0.30 \text{ V vs. SCE}$ , respectively, while DADCQ reduces at  $+0.45 \text{ V vs. SCE}$ . These values demonstrate that (i) HNS is only a weak acceptor, comparable to trinitrofluorenone ( $E_{\text{red}} = -0.45 \text{ V vs. SCE}$ ) or benzoquinone ( $E_{\text{red}} = -0.51 \text{ V vs. SCE}$ ), and (ii) TAZQ, albeit a better acceptor than the parent benzoquinone, reduces at a potential inferior to that of chloranil ( $+0.01 \text{ V vs. SCE}$ ). Thus, we deduce that the electron-withdrawing capability of the azido group is slightly inferior to that of chlorine or bromine substituents. As a consequence the reduction potential of DADCQ is dominated by the strongly electron-withdrawing cyano groups and is only lowered by 60 mV when compared with the reduction potential of DDQ (dichlorodicyanoquinone,  $+0.51 \text{ V vs. SCE}$ ).

Thus, with the oxidation potential of TTF at  $+0.33 \text{ V vs. SCE}$ , we expect HNS and TAZQ to form neutral charge-transfer complexes while DADCQ should oxidize TTF to the corresponding cation radical. The complexes were prepared by mixing equimolar (1 mM)  $\text{CH}_3\text{CN}$  solutions of the donor and acceptor. Black precipitates of 1:1 stoichiometry were obtained:  $\text{TTF} \cdot \text{TAZQ}$ ,  $\text{TTF} \cdot \text{HNS}$  and  $\text{TTF} \cdot \text{DADCQ}$ . From these complexes, single crystals suitable for X-ray structural analysis could be grown for  $\text{TTF} \cdot \text{HNS}$  and  $\text{TTF} \cdot \text{TAZQ}$  only by slow diffusion in a  $\text{CH}_3\text{CN}:\text{DMSO}$  mixture.

In the following we will concentrate on the structural and optical properties of the two crystalline materials obtained so far during this work,  $\text{TTF} \cdot \text{HNS}$  and  $\text{TTF} \cdot \text{TAZQ}$ .

### Structural properties

$\text{TTF} \cdot \text{TAZQ}$  crystallises in the monoclinic system, space group  $P2_1/n$ . Both components are located on an inversion center and are fully planar (Fig. 1). As observed in structures containing aryl azide groups,<sup>13,14</sup> the  $\text{C}-\text{N}_\alpha-\text{N}_\beta$  angles lie

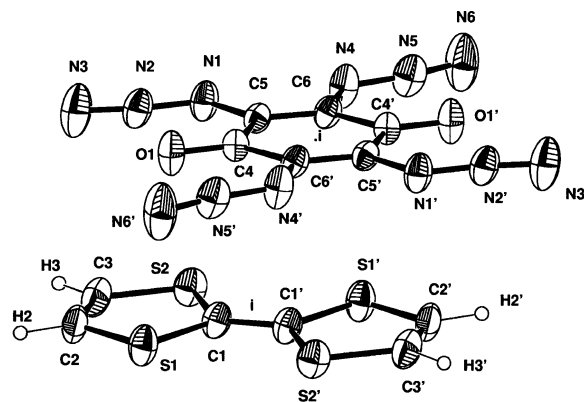
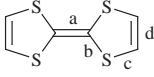


Fig. 1 ORTEP drawing and numbering scheme for  $\text{TTF} \cdot \text{TAZQ}$

around  $120^\circ$  while the azido groups themselves are not completely linear but present an averaged  $\text{N}_\alpha-\text{N}_\beta-\text{N}_\gamma$  angle value of  $167^\circ$ . The expected quinoid structure is observed for the central six-carbon ring with a bond length alternation of 1.336(6) and 1.479(6) Å. Bond distances within the TTF moiety are known to be sensitive to the degree of charge transfer (Table 1). The values observed here in  $\text{TTF} \cdot \text{TAZQ}$  are indicative of the presence of a *neutral* TTF molecule. In the solid, stacks of alternating donor and acceptor molecules develop along the  $b$  axis, at the corners and the center of the unit cell. The plane-to-plane distance amounts to 3.361(4) Å while the parallel donor and acceptor planes make an angle of  $21.8^\circ$  with the  $b$  stacking axis. The overlap between donor and acceptor molecules is shown in Fig. 2 and appears to be com-

Table 1 Bond distances of the TTF molecule in various TTF salts. The estimated errors on the averaged distances are calculated from  $\sigma(d_{\text{mean}}) = [\sum(d_i - d_{\text{mean}})^2/(n-1)]^{1/2}$

Bond				
	TTF <sup>a</sup>	TTF · HNS	TTF · TAZQ	TTF · ClO <sub>4</sub> <sup>b</sup>
a	1.349(3)	1.342(7)	1.356(7)	1.404(5)
b	1.757(1)	1.76(1)	1.750(6)	1.713(7)
c	1.726(4)	1.74(1)	1.738(4)	1.72(1)
d	1.314(3)	1.321(8)	1.322(6)	1.31(1)

<sup>a</sup> Ref. 15. <sup>b</sup> Ref. 16.

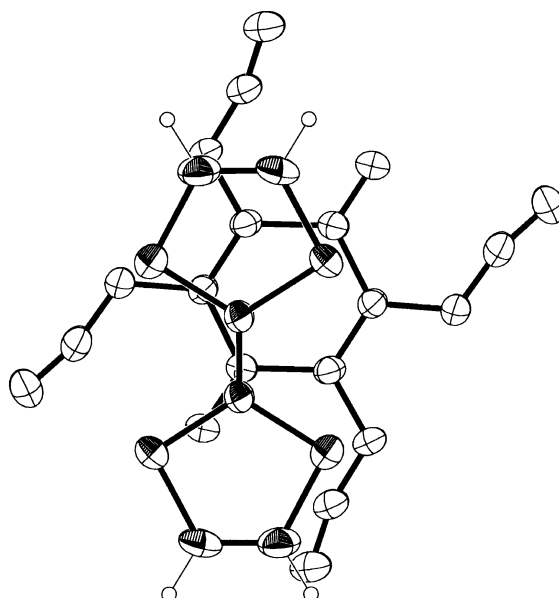


Fig. 2 Projection view of the overlap of TTF with TAZQ

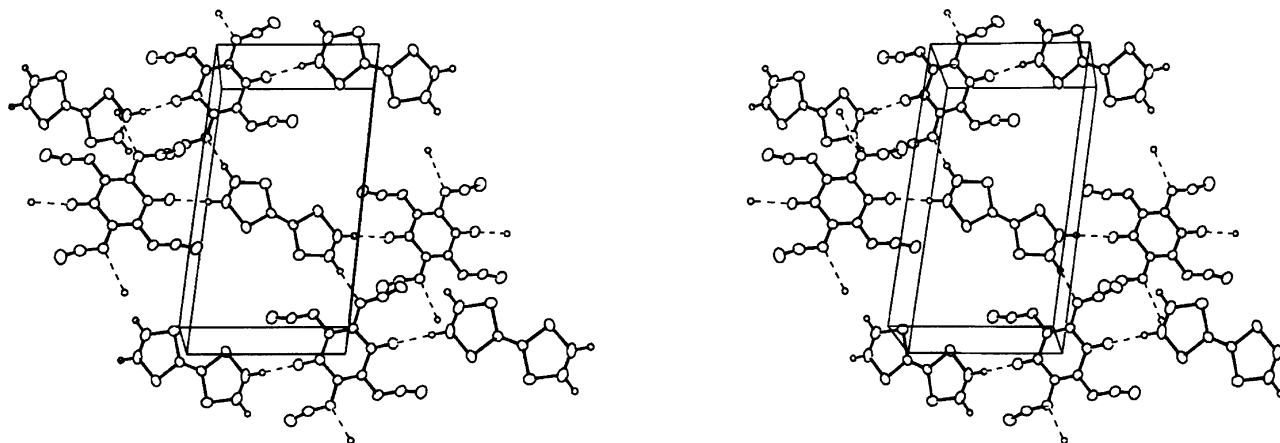


Fig. 3 Stereoview of the unit cell, showing the hydrogen-bonded network in TTF · TAZQ

parable with the one observed in TTF·chloranil and TTF·fluoranil complexes.<sup>11</sup> One of the internal TTF C—S bonds is located directly over the quinoid ring with the sulfur atom closest to the electron-poorest carbonyl carbon atom, in accordance with recently developed calculations on  $\pi$ – $\pi$  interactions.<sup>17</sup>

Furthermore, the cohesion of the whole structure is achieved through a polymeric network of C—H $\cdots$ X (X = O, N) interactions (Fig. 3). Indeed, each hydrogen atom of the TTF moiety is engaged in such a bond, H2 with the quinoid oxygen atom of TAZQ and H3 with the N4 nitrogen atom (N<sub>4</sub>) of the azido group. These bonds exhibit the characteristic features of C—H $\cdots$ X bonds<sup>18</sup> with C2 $\cdots$ O1 and C3 $\cdots$ N4 distances of 3.333(6) and 3.534(9) Å and C2—H2 $\cdots$ O1 and C3—H3 $\cdots$ N4 angles of 170.1(3) and 143.4(3)°, respectively. The strongest C2—H2 $\cdots$ O1 bond leads to the formation of infinite —TTF—TAZQ—TTF—TAZQ— chains in the  $a + b$  and  $a - b$  directions, crosslinked by the C3—H3 $\cdots$ N4 interaction, which develops in the  $c$  direction. This arrangement is represented as N<sub>1</sub>:C<sub>2</sub>(14)C<sub>2</sub>(14) using the graph sets proposed by Etter.<sup>19</sup>

TTF·HNS crystallises in the monoclinic system, space group  $P2_1$  (Fig. 4). Both components are in a general position in the unit cell. Bond distances in the TTF moiety here are also indicative of a neutral state (Table 1) while the TTF molecule adopts a chair conformation with a bending of the dithiole rings along the S—S axis, by 7.5(5)° along S1—S2 and by 8.0(5)° along S3—S4. The HNS molecule is not planar, as already observed in the structure of HNS itself.<sup>20</sup> The two trinitrophenyl moieties are located in parallel planes and linked by the ethylene bridge with dihedral angles of 60.35 and 68.47° with the plane containing the ethylenic bridge, values to be compared with 67.11 and 72.0° in neutral HNS. Also, the ethylenic carbon atoms are located slightly outside the plane of the benzenic rings, by 0.129(6)Å for C7 and 0.022(6)Å for C8. Those strong distortions from planarity, as already discussed for HNS itself, are mainly attributable to the presence of bulky nitro groups in positions *ortho* to the ethylenic bridge. As a consequence the molecule then distorts along the double bond and two of the *ortho* nitro groups are severely rotated out of the phenyl rings, by 46 and 42°. Internal bond lengths and angles are in the range of those reported for HNS. In the complex, an alternating stack forms along the  $b$  axis with TTF and one half of a HNS molecule, with an averaged intrastack interplanar spacing between donor and acceptor of 3.40 Å. In addition the donor and acceptor planes make an angle of 21° with the  $b$  axis. The overlap pattern is shown in Fig. 5; the two nitro groups overlapping with the TTF moieties are nearly eclipsed with the phenyl ring.

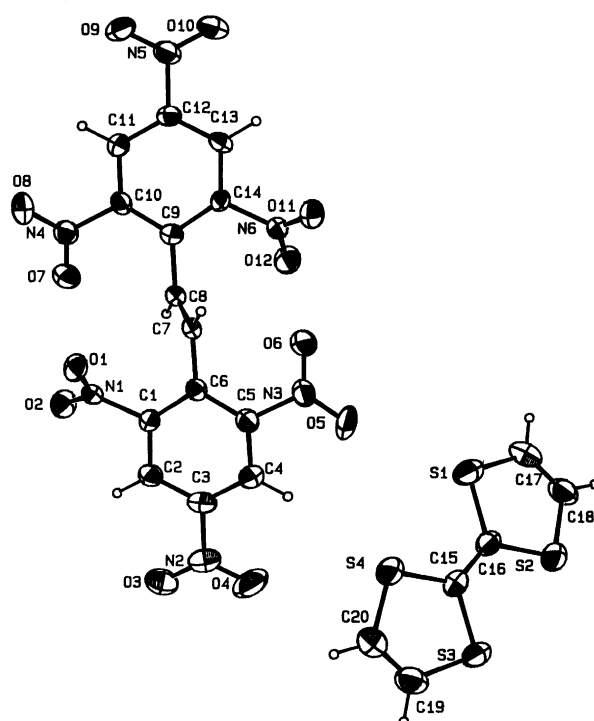


Fig. 4 ORTEP drawing and numbering scheme for TTF · HNS

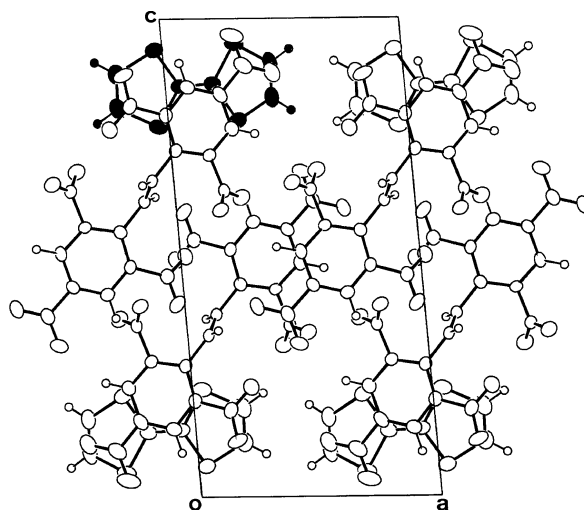
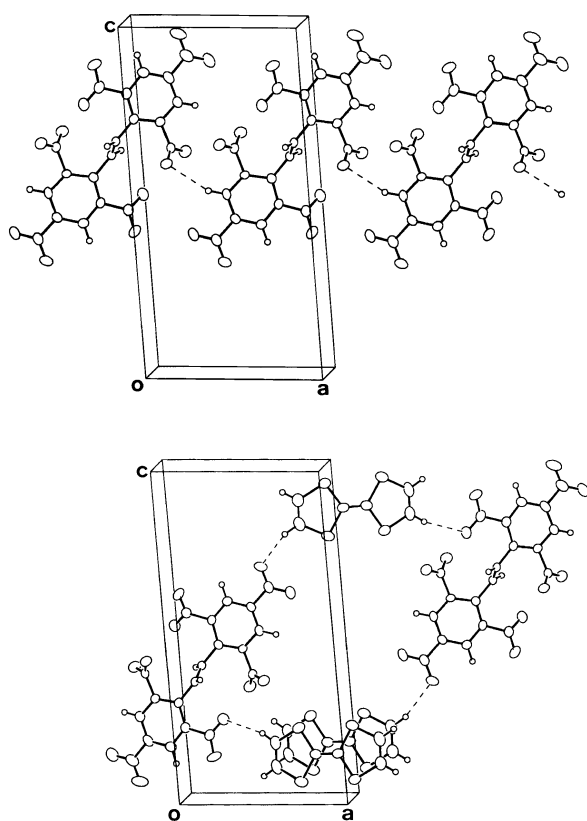


Fig. 5 A projection view of the TTF · HNS unit cell along (010), showing the overlap of TTF with HNS

**Table 2** Geometrical characteristics of C—H...O hydrogen bonds in HNS · TTF

	C...O distance/Å	C—H...O angle/°
HNS...HNS: C13—H13...O1	3.523(6)	158.0(3)
HNS...TTF: C19—H19...O9	3.400(7)	144.2(4)
C18—H18...O6	3.457(7)	165.4(4)

Superimposed on the DADADA alternating structure along *b*, one also identifies a C—H...O hydrogen-bonded network, which develops in the *a* and *b* directions of the crystal. Indeed, examination of the shortest C—H...O intermolecular contacts shows that one hydrogen atom, H13, of HNS and two hydrogen atoms of TTF, H18 and H19, are engaged in such short interactions with the oxygen atoms of neighbouring nitro groups (Table 2). The HNS...HNS interaction develops in the *a* direction and is identified using graph sets as  $N_1 =$



**Fig. 6** The hydrogen-bonded network in TTF · HNS. Top: the chain along (100) through HNS–HNS interactions. Bottom: the helix around (010) through TTF–HNS interactions

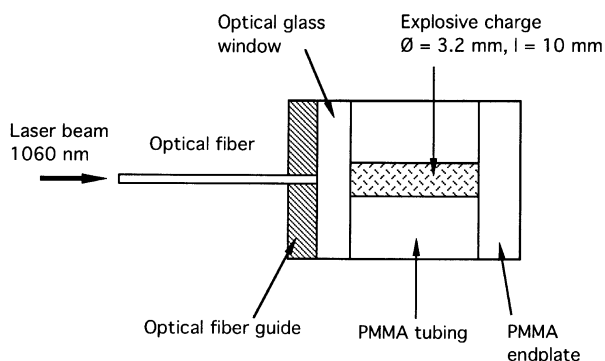


**Fig. 7** Experimental set-up to test laser ignition

C10 (Fig. 6, top) while the two HNS...TTF interactions ( $N_1 = DD$ ) lead to a helical structure around the polar *b* axis (Fig. 6, bottom). As a consequence, the whole structure is tightly arranged in the *a* and *b* directions within layers while only van der Waals interactions can be expected between those *ab* layers, in the *c* direction.

### Optical and detonant properties

As already mentioned, the large difference between the oxidation potential of TTF and the reduction potentials of HNS or TAZQ provides a rationale for the observation of bond distances in the TTF moieties characteristic of a *neutral* TTF molecule. This is substantiated by the absence of any EPR signal at room temperature on single crystals of both compounds, which can be then considered as neutral molecular complexes.

A charge-transfer absorption band was observed between 900 and 1200 nm ( $\lambda_{\text{max}} = 1100$  nm) in TTF · TAZQ and TTF · DADCQ but no noticeable extra band could be detected in the spectrum of TTF · HNS, besides those of neutral TTF and HNS. This charge-transfer band energy confirms that the TAZQ and DADCQ complexes with TTF are appropriate candidates for an NIR light-induced activation.

Preliminary experiments on light-induced decomposition have been conducted on the TTF · DADCQ complex. The product was charged at natural density in a PMMA tube of 3.2 mm i.d. and 10 mm long between a PMMA endplate and an optical glass window (Fig. 7). A laser pulse (1.06  $\mu\text{m}$  wavelength, 20 ns duration) was applied *via* an optical fiber onto the glass window. Total decomposition of the complex was observed, however without detonation. A small print was noted on the rear plate. This first result confirms our initial assumptions that a strong optical absorption of the product at the laser wavelength indeed greatly enhances decomposition by the laser pulse. Transition to detonation might be attained in other experimental configurations, for example by increasing the charge dimensions over the critical diameter.

## Experimental

### Synthesis

TTF was prepared according to published procedures<sup>21</sup> and sublimed under vacuum before use. TAZQ<sup>22</sup> and DADCQ<sup>23</sup> were prepared following published procedures. *Caution: TAZQ and DADCQ have already been described as being extremely sensitive to friction and impact and should be handled with due precautions in only very small quantities.*

Charge-transfer complexes were prepared by mixing hot equimolar solutions (1 mM) of TTF and the acceptor (HNS, TAZQ or DADCQ) in  $\text{CH}_3\text{CN}$ . Slow cooling to room temperature and further cooling to 0 °C overnight produced needle-like crystals, which were collected by filtration and washed with cold  $\text{CH}_3\text{CN}$ . *Caution: while TTF · HNS appears to be stable under normal conditions, crystals of TTF · TAZQ decompose spontaneously at room temperature and were better stored in very small quantities in a refrigerator. Caution: TTF · TAZQ and TTF · DADCQ are extremely sensitive to friction and impact and should be handled with due precautions in only very small quantities.*

### X-ray studies

A single crystal of TTF · HNS was fixed at the end of a glass fiber with epoxy glue while a single crystal of TTF · TAZQ was completely covered with a thin layer of epoxy glue cement in order to avoid the spontaneous decomposition observed with uncovered crystals. Precise unit cell dimensions and intensity data were collected on an Enraf-Nonius CAD4-F diffractometer, using graphite-monochromated Mo-K $\alpha$  radi-

**Table 3** Crystallographic data for TTF · HNS and TTF · TAZQ

	TTF · HNS	TTF · TAZQ
Formula	C <sub>20</sub> H <sub>10</sub> N <sub>6</sub> O <sub>12</sub> S <sub>4</sub>	C <sub>12</sub> H <sub>14</sub> N <sub>12</sub> O <sub>2</sub> S <sub>4</sub>
Formula weight	654.57	476.50
Crystal dimensions/mm	0.36 × 0.12 × 0.06	0.30 × 0.12 × 0.10
Crystal color	Shiny black	Shiny black
T/K	293	293
Crystal system	Monoclinic	Monoclinic
Space group	P2 <sub>1</sub>	P2 <sub>1</sub> /n
a/Å	9.193(1)	8.295(1)
b/Å	7.428(2)	7.242(3)
c/Å	18.350(2)	14.984(2)
β/deg	94.507(9)	96.26(1)
U/Å <sup>3</sup>	1249(1)	894.8(4)
Z	2	2
D <sub>calc</sub> /g cm <sup>-3</sup>	1.741	1.769
μ/cm <sup>-1</sup>	4.4	5.5
Scan type	ω – 2θ	ω – 2θ
Scan width/deg	1 + 0.35 tan θ	1 + 0.35 tan θ
Absorption correction	None	ψ scans
2θ <sub>max</sub> /deg	52	52
Data collected	2830	1816
Independent data	2656	1682
Observed data [ <i>I</i> <sub>obs</sub> ≥ 3σ( <i>I</i> )]	1837	937
Parameters refined	378	136
<i>R</i> <sup>a</sup>	0.043	0.048
<i>R</i> <sub>w</sub> <sup>b</sup>	0.043	0.055
Goodness-of-fit	1.21	1.756
Final shift/error	0.0	0.0
Res. dens/e Å <sup>-3</sup>	0.29, –0.34	0.48, –0.42

$$^a R = \Sigma ||F_o| - |F_c|| / \Sigma |F_o|, ^b R_w = \Sigma_w (|F_o| - |F_c|)^2 / \Sigma_w |F_o|^2]^{1/2}, w = 4F_o^2 / [\sigma^2(I) + (0.04F_o^2)^2]$$

**Table 4** Important bond distances/Å in TTF · HNS

C6—C7	1.487(6)	S3—C15	1.762(5)
C7—C8	1.321(7)	S3—C19	1.751(6)
C8—C9	1.488(6)	S4—C15	1.757(5)
S1—C16	1.771(5)	S4—C20	1.730(7)
S1—C17	1.751(7)	C15—C16	1.342(7)
S2—C16	1.742(5)	C17—C18	1.315(9)
S2—C18	1.732(7)	C19—C20	1.327(9)

**Table 5** Important bond distances/Å and angles/° in TTF · TAZQ

S1—C1	1.745(4)	N1—C5	1.386(4)
S1—C2	1.741(4)	N2—N3	1.114(4)
S2—C1	1.754(4)	N4—N5	1.258(4)
S2—C3	1.735(4)	N4—C6	1.396(4)
C1—C1'	1.356(7)	N5—N6	1.118(4)
C2—C3	1.322(6)	C4—C5	1.476(5)
O1—C4	1.215(4)	C4—C6	1.483(5)
N1—N2	1.252(4)	C5—C6	1.336(5)
N2—N1—C5	119.8(3)	N4—N5—N6	167.4(4)
N1—N2—N3	166.7(4)	N5—N4—C6	120.3(3)

ation ( $\lambda = 0.71073$  Å). The structures were solved by MULTAN and successive Fourier differences. Hydrogen atoms were introduced at calculated positions, included in structure factor calculations but not refined (riding model). All computer programs are from the Enraf-Nonius structure determination package. Crystal data, details of the data collection and structure solving are listed in Table 3; selected bond distances and angles for TTF · HNS and TTF · TAZQ are given in Tables 4 and 5, respectively. CCDC reference number 440/036.

## Acknowledgements

We thank the French Government STPE (DGA) for financial support. S. Lecume is gratefully acknowledged for performing the laser tests.

## References

- (a) D. A. Benson and B. H. Rose, in *Proceedings of the 13th International Pyrotechnics Symposium*, ITT Research Institute, Chicago, 1988, p. 49. (b) D. J. Lewis, in *Proceedings of the 5th Symposium on Electroexplosive Devices*, Distributed by National Technical Information Service, US Department of Commerce, Springfield, VA, 1967, pp. 1–8.1.
- D. W. Ewick, L. R. Dosser, S. R. McComb and L. P. Brodsky, in *Proceedings of the 13th International Pyrotechnics Symposium*, ITT Research Institute, Chicago, 1988, p. 263.
- G. Krassoulia, in *Proceedings of the 3rd International Congress of Spatial Pyrotechnics*, Association Française de Pyrotechnie, Paris, 1987, p. 135.
- M. Folsom, in *Proceedings of the 14th Symposium on Explosives and Pyrotechnics*, ed. Franklin Research Center, US, 1990, pp. XVIII.1–XVIII.18.
- (a) S. C. Kunz and F. J. Salas, in *Proceedings of the 13th International Pyrotechnics Symposium*, ITT Research Institute, Chicago, 1988, p. 505. (b) L. C. Yang, *Propellants, Explosives Pyrotech.*, 1981, **6**, 151. (c) D. L. Paisley, in *Proceedings of the 9th International Symposium on Detonation*, ed. W. J. Morat, Office of Naval Research, 1989, p. 492. (d) A. M. Renlund, P. L. Stanton and W. M. Trott, *ibid.*, p. 781. (e) A. Delpuech, *ibid.*, p. 73. (f) S. Chengwei, W. Zuoni, F. Qing, C. Danming and L. Yultun, in *Proceedings of the International Symposium on Intense Dynamic Loading and its Effects*, Pergamon, Oxford, 1986, p. 192. (g) J. Baoren, in *Proceedings of the International Symposium on Pyrotechnics and Explosives*, ed. D. Jing, China Academic Publishers, Beijing, 1987, p. 49. (h) E. I. Alexandrov, A. G. Voznyuk and V. P. Tsipilev, *Comb. Expl. Shock Waves*, 1989, **25**, 1. (i) B. L. Feltherolf, T. S. Snyder, M. D. Bates, A. Peretz and K. K. Kuo, in *Proceedings of the 14th International Pyrotechnics Symposium*, 1989, p. 691. (j) L. V. de Yong and F. J. Valenta, *ibid.*, p. 123. (k) P. S. Henning and M. D. Brown, *ibid.*, p. 495. (l) E. I. Alexandrov and A. G. Voznyuk, *Comb. Expl. Shock Waves*, 1988, **24**, 730.
- (a) J. W. Fronabarger, W. B. Sanborn and T. Massis, in *Proceedings of the 22nd International Pyrotechnics Seminar*, ITT Research Institute, Chicago, 1996, p. 645. (b) J. W. Fronabarger, W. B. Sanborn, T. Massis, A. Schuman, R. D. Chapman and W. Fleming, in *Proceedings of the International Symposium on Energetic Materials Technology*, American Defense Preparedness Association, Washington, DC, 1994, p. 254. (c) J. W. Fronabarger, W. B. Sanborn and J. Q. Searcy, in *Compatibility of Plastics/ Materials with Explosives—Explosives Processing*, American Defense Preparedness Association, Washington, DC, 1979, p. 238.

- 7 K. J. Smit, *J. Energetics Mater.*, 1991, **9**, 81.
- 8 F. H. Herbstein, *Persp. Struct. Chem.*, 1971, **4**, 166.
- 9 J. B. Torrance, *Acc. Chem. Res.*, 1972, **12**, 79.
- 10 J. B. Torrance, B. A. Scott and F. B. Kaufman, *Solid State Commun.*, 1975, **17**, 1369.
- 11 J. J. Mayerle, J. B. Torrance and J. I. Crowley, *Acta Crystallogr., Sect. B*, 1979, **35**, 2988.
- 12 (a) P. Batail, S. J. LaPlaca, J. J. Mayerle and J. B. Torrance, *J. Am. Chem. Soc.*, 1981, **103**, 951. (b) J. B. Torrance, A. Girlando, J. J. Mayerle, J. I. Crowley, V. Y. Lee, P. Batail and S. J. LaPlaca, *Phys. Rev. B*, 1981, **47**, 1747.
- 13 U. Müller, in *Structure and Bonding*, ed. J. D. Dunitz, Springer, Berlin, 1973, vol. 14, pp. 141–172.
- 14 See also as examples: (a) A. Schulz, I. C. Tornieporth-Oetting and T. M. Klapötke, *Angew. Chem., Int. Ed. Engl.*, 1993, **32**, 1610. (b) A. Mugnoli, C. Mariani and M. Simonetta, *Acta Crystallogr.*, 1965, **19**, 367. (c) A. S. Bailey and C. K. Prout, *J. Chem. Soc.*, 1965, 4867.
- 15 W. F. Coppins, N. C. Kenney, J. C. Edmonds, A. Nagel, F. Wudl and P. Coppins, *J. Chem. Soc., Chem. Commun.*, 1971, 889.
- 16 K. Yakushi, S. Nishimura, T. Sugano and H. Kuroda, *Acta Crystallogr., Sect. B*, 1980, **36**, 358.
- 17 C. A. Hunter and J. K. M. Sanders, *J. Am. Chem. Soc.*, 1990, **112**, 5525.
- 18 (a) R. Taylor and O. Kennard, *J. Am. Chem. Soc.*, 1982, **104**, 5063. (b) G. R. Desiraju, *Acc. Chem. Res.*, 1991, **24**, 290.
- 19 (a) M. C. Etter and J. C. MacDonald, *Acta Crystallogr., Sect. B*, 1990, **46**, 256. (b) M. C. Etter, *Acc. Chem. Res.*, 1990, **23**, 120.
- 20 F. Gérard and A. Hardy *Acta Crystallogr., Sect. C*, 1988, **44**, 1283.
- 21 L. R. Melby, H. D. Hartzler and W. A. Sheppard, *J. Org. Chem.*, 1974, **39**, 2456.
- 22 W. H. Gilligan and M. J. Kamlet, *Tetrahedron Lett.*, 1978, 1675.
- 23 (a) R. Neidlein, W. Kramer and R. Leidholdt, *Helv. Chim. Acta*, 1983, **66**, 652. (b) R. Neidlein and R. Leidholdt, *Chem. Ber.*, 1986, **119**, 844.

*Received in Montpellier, France, 6th November 1997;  
Paper 7/09257A*